SUPPLEMENTARY MATERIAL

NMR-based metabolomic profiling of the differential concentration of phytomedicinal compounds in pericarp, skin and seeds of Momordica charantia (bitter melon)

Sumit Mishra[a], Ankit[a], Rakesh Sharma[a], Navdeep Gogna[a b] and Kavita Dorai[a*]

[a]*Department of Physical Sciences, Indian Institute of Science Education & Research (IISER) Mohali, Sector 81 SAS Nagar, Manauli PO 140306 Punjab India.*

[b]*MDI Biological Laboratory, Bar Harbor, ME 04609, USA.*

*Corresponding Author
Email address: **kavita@iisermohali.ac.in** (Kavita Dorai)
Tel & Fax: +91-172-2240266

ABSTRACT

Momordica charantia is a medicinal plant which is widely used in traditional medicine (Indian ayurvedic and Chinese herbal) to treat several diseases. We have identified the differential distribution of phytomedicinally important metabolites in the pericarp, skin and seeds of Momordica charantia fruit via ^{1}H nuclear magnetic resonance (NMR) spectroscopy. Orthogonal partial least-squares-discriminant analysis (OPLS-DA) showed a clustering of the metabolic profiles of seeds and pericarp (indicating their similarity) and their clear separation from the metabolic profile of the skin. The total phenolic content and total flavonoid content of the fruit extracts were estimated via bioassays, the radical scavenging activity were estimated via in vitro DPPH and ABTS assays and an inhibitory activity test of α-glucosidase was performed in vitro via a spectrophotometric method. The pericarp and seeds contained significantly higher amounts of phenolic compounds and flavonoids, indicating that they can be used as a good source for antioxidants. The skin contained a significantly higher amount of phytosterols such as Charantin and momordicine, which are known to correlate with antidiabetic activity.

KEYWORDS

^{1}H NMR spectroscopy; Metabolite fingerprinting; Momordica charantia; Phytomedicinal compounds; Antioxidant activity

Experimental Methods

Materials

Organic M. charantia mature fruits (picked approximately 3-4 weeks post-flowering) were bought from the market. Ten M. charantia mature fruits approximately 8×3 cm were chosen for the study. The skin, pericarp and seeds of the mature fruit was green, white and yellowish in color respectively, and the seeds were completely developed (figure S1 in supplementary material for details). The fruits of M. charantia used in this study was collected by Sumit Mishra from local market (latitude 30.68110 N & longitude 76.74660 E) of Mohali (Panjab) in October 2019. The voucher specimen (Accession Number: 2020/MT04/0001) was deposited at the NMR research facility IISER Mohali, Panjab (figure S2 in the supplementary material).

Chemicals and reagents

All extraction solvents, reagents, NMR reference standards and deuterated solvents were of analytical grade with purity greater than 90% and were procured from Sigma Aldrich (India). Deuterium oxide (D_2O, 99.9%) and deuterated methanol-D4 (CD_3OD-D_4, 99.80%) were used as the deuterated solvents. Trimethylsilane propionic acid sodium salt (TMSP) was added as an internal standard for all ^1H NMR measurements. Sodium azide (NaN_3, 99.5%) and phosphate buffer solution (2.0 mM, pH 7.4) were used in this study. Metabolite extraction from M. charantia was performed at room temperature using CD_3OD and D_2O as extraction solvents via standard protocols (Fan et al. 2014).

NMR sample preparation

Ten replicates from the individual fruits were analyzed for each type of sample: skin, pericarp and seeds. The fruits were surface cleaned by washing them with distilled water to remove all debris and dried with tissue paper. The pericarp, seeds were removed, and the skin was cut into thin pieces. Then the samples were ground in liquid nitrogen using a mortar and pestle and kept in separate air-tight plastic containers. These samples were then stored overnight at -80 ^{0}C. All the samples were then lyophilized using a freeze dryer at a pressure of 30 Pa for 16 h at -40 ^{0}C. NMR samples were prepared by taking 25 mg of dried skin, pericarp and seed powder mixed thoroughly with the solvents containing 320 µL of methanol-D4, 180 µL of D_2O (phosphate

buffered saline, pH 7.4 made in D_2O), 100 µL of sodium azide (to prevent bacterial growth), and 2mM trimethylsilane propionic acid sodium salt (TMSP) as an internal reference. Then 600 µL solution was vortexed and centrifuged at 5000 g for 5 min and 500 µL of the filtered supernatant was used for the NMR experiments.

NMR spectroscopy

All NMR experiments were performed at 298 K on a Bruker Biospin 600 MHz Avance III spectrometer operating at a proton resonance frequency of 600.219 MHz, equipped with a 5 mm QXI quadrupolar resonance probe. Methanol-d4 was used as an internal lock and gradient shimming was performed prior to signal acquisition. For ^{1}H NMR spectra acquisition, a water suppressed Carr-Purcell-Meiboom-Gill (CPMG) spin-echo pulse sequence optimized with a spin-echo delay τ of 300 µs and loop counter n = 400 and a total spin-spin relaxation delay time ($2n\tau$) of 240 ms was used to attenuate the background broad signals from large molecules. The proton spectra were collected with a 90-degree pulse width of 9.95 µs, a relaxation delay of 4 s, 8 scans, 64 K data points and a spectral width of 12 ppm. Data were zero-filled by a factor of 2 and the FID's were multiplied by an exponential weighting function equivalent to a line broadening of 0.3 Hz prior to Fourier transformation. The NMR spectra were phase and baseline-corrected and trimethylsilane propionic acid sodium salt (TMSP) was added to provide an internal NMR reference at 0.00 ppm. To confirm the peak assignments, 2D NMR experiments were recorded, including homonuclear ^{1}H-^{1}H correlation spectroscopy (COSY), total correlation spectroscopy (TOCSY) and heteronuclear ^{1}H-^{13}C coherence spectroscopy (HSQC). 2D COSY and TOCSY spectra were recorded with a spectral width of 12 ppm in both the proton F1 and F2 dimensions, 2K data points, 16 scans and 128 t_1 increments. 2D HSQC spectra were acquired with a spectral width of 12 ppm and 200 ppm in proton and carbon dimensions, respectively, 1K data points, 32 scans and 128 t_1 increments.

Metabolite identification

The metabolites were identified using both 1D and 2D NMR experiments and also from comparing the obtained chemical shift and coupling constant values with standard NMR metabolite peaks from databases such as Biological Magnetic Resonance Data Bank (BMRB) (http://www.bmrb.wisc.edu), the Madison Metabolomics Consortium Database (MMCD) (http://mmcd.nmrfam.wisc.edu/) and the Human Metabolite Data Base (HMDB)

(http://www.hmdb.ca/). Pure beta-sitosterol and stigmasterol were recorded in deuterated chloroform and used as a reference to identify peaks in the NMR spectra of M. charantia. We tried to record the NMR spectra of as many pure compounds as possible such as chlorogenic acid, gamma-aminobutyric acid (GABA), quinic acid, sucrose, tryptophan and vanillic acid (recorded in a mixture of deuterated methanol-D4 and D_2O). The ^1H NMR data of the pure compounds are given in Figures S4-S11 (supplementary material). We used the metabolomics standards initiative (MSI) (Sumner et al. 2007) to classify the identified metabolites: as belonging to MSI level 1 if two or more independent and orthogonal parameters are identical to those of a reference compound interpreted under the same conditions (for instance through 1D ^1H and 2D HSQC NMR spectra). If this information is not available the metabolite is putatively annotated from publications, databases or libraries and categorized as belonging to MSI level 2. The MSI level for each metabolite is given in the supplementary material.

Multivariate statistics

The NMR data were converted to ASCII format and aligned using the icoshift (interval correlation shifting) MATLAB algorithm (Savorani et al. 2010). Further NMR data analysis was performed using MestReNova software version 10.0.2-15465 (Mestrelab Research, Spain). The spectra were subdivided in the range 0.02 to 10.0 ppm and binned into regions of equal spectral width (0.01 ppm), referenced to a peak of TMSP. Data were normalized to a total integral of 100. The spectral region δ 4.60 − 5.12 ppm contained residual water peaks and was not considered for the analysis. Prior to the chemometric analysis, all the data sets were Pareto-scaled. Principal component analysis (PCA), Orthogonal projections to latent structures discriminant analysis (OPLS-DA), one-way analysis of variance (ANOVA), statistical Student's t-tests, and hierarchical clustering heat map analysis were performed using SIMCA version 14.1.0-2047 software (Umetrics, Umea, Sweden) and Metaboanalyst software (http://www.metaboanalyst.ca/). For detection of outliers, PCA was first performed and data points located outside the 95 % confidence region of the Hotelling's ellipse in the PCA score plot, were removed from the subsequent OPLSDA analysis. The quality of the OPLS-DA model was assessed from the R^2Y (variance predicted) and Q^2 (variance explained) values. The separation between the groups were observed using the OPLS-DA scores plot, having one predictive and one orthogonal component. Significant metabolites, responsible for group separation were identified from the S-plot and Student's t-test and p-values $\leq$ 0.05 and 0.01 respectively, were considered significant. Metabolomic pathway analysis was constructed

using the MetPA web-based tool (http://www.metaboanalyst.ca). The highest impact value was obtained for the flavone and flavonol synthesis (impact value = 0.8, FDR p-value < 0.05). Metabolic pathways including: flavonoid biosynthesis, phenylpropanoid biosynthesis, aminoacyl-tRNA biosynthesis, sulfur metabolism, cysteine and methionine metabolism, butanoate metabolism, alanine, aspartate and glutamate metabolism were statistically significant (impact value ≥ 0.005, FDR p-value < 0.05).

Quantifying total phenolic content

The total phenolic content in pericarp, skin and seeds of M. charantia was quantified using the Folin-Ciocalteu spectrophotometric method (Gogna et al. 2015). The fruit extract (1.0 mL of methanol extraction) was mixed in a vial with 5 mL of Folin-Ciocalteu phenol reagent (diluted 10 times with distilled water). After 5 minutes, 5 mL of 7.5% Na_2CO_3 solution was mixed and the vials were kept for 20 minutes at 25 ^{0}C to complete the reaction. The absorbance was measured on the UV-Vis spectrophotometer at 760 nm at room temperature. The standard curve was prepared using gallic acid. The total phenolic content for each type of extract (pericarp, skin and seed) was expressed as milligrams of gallic acid equivalent (mg GAE) per g of dried weight sample (g DW). All measurements were performed thrice and the results were averaged.

Quantifying total flavonoid content

The total flavonoid content in different parts of the M. charantia L. was quantified by the method described by (Zhou et al. 2011). 1 mL of fruit extract (methanol extraction) was mixed in a vial with 6 mL of distilled water, 200 µL of aluminum chloride solution and 200 µL of potassium acetate solution. The mixture was allowed to stand for 30 min. at 25 ^{0}C to complete the reaction. The absorbance was measured at 510 nm using a UV-Vis spectrophotometer. The total flavonoid content was calculated from a calibration curve obtained using a standard solution of quercetin, and the result was expressed as mg quercetin equivalent (mg QE) per g of dry weight sample (g DW). All measurements were performed thrice and the results were averaged.

Quantifying free radical scavenging activity

Free radical scavenging activity was measured from a 2,2-diphenyl-1-picrylhydrazyl (DPPH) assay using the method described by (Meda et al. 2005), wherein 4 mg of fruit extract was dissolved in 10 mL of methanol to prepare a 400 µg/mL solution and then serial dilution was performed to prepare the required concentrations. As a positive control, 2 mg of quercetin (12.5 - 400 µg/ml) was dissolved in 2.5 mL distilled water. 1 mL of methanol solution of fruit extract/standard of different concentrations was mixed in a vial with 3 mL of methanol solution of DPPH and incubated at room temperature for 30 minutes in the dark. Absorbance of the solution was recorded at 517 nm using a UV-Vis spectrophotometer. The DPPH radical scavenging capacity (SC %) was calculated as:

$$SC\ (\%) = [(A_0 - A_s)/A_0] \times 100$$

where A_0 is the absorbance of the reagent blank and A_s is the absorbance of the samples. The results were expressed as EC_{50} (the half maximal effective concentration), which denotes the concentration of the sample required to scavenge 50% of the DPPH free radicals. A stoichiometric change in color occurs during the conversion from a DPPH free radical to reduced DPPH-H

$$DPPH' + A\text{-}H \rightarrow DPPH\text{-}H + A'$$

It was observed that the purple color of DPPH was reduced upon treatment with the M. charantia extracts at all the tested concentrations. The scavenging activity increases with the increase in concentrations up to 400 µg/mL for the extracts, after which a plateau is reached, as seen in supplementary material figure S28 (b). The antioxidant activity of plants has been attributed to the presence of phenolic compounds which have the ability to lose protons and can hence contribute to radical scavenging. The results of the DPPH assay corroborate those obtained from evaluating the total phenolic content. Seed extracts of M. charantia, which had the highest total phenolic content also showed the highest antioxidant activity.

Quantifying radical cation scavenging activity

Antioxidant activity of M. charantia extracts fruit extracts with the 2,2′-azino-bis(3-ethylbenzothiazoline-6-sulphonic acid) diamonium salt (ABTS+) cation radical was measured using the method reported by Rajurkar et. al. with some modifications (Rajurkar and Hande 2011). A stock solution of ABTS+ radical was prepared by mixing ABTS (7 mM) with potassium persulfate (2.45 mM) in distilled water. The solution was kept in the dark at room temperature for 12-16 hours before use, and then diluted with methanol to obtain an absorbance of 0.70 ± 0.02 units at 734 nm on the UV-Vis spectrophotometer. Methanol fruit extracts (10 µL of each sample) were mixed thoroughly with 2.99 mL of the ABTS+ stock solution in a cuvette in the dark, and the decrease in the absorbance was measured after 1 hour. The standard curve was obtained using 2 mg Trolox (6-hydroxy-2,5,7,8-tetramethylchroman-2-carboxylic acid) dissolved in 2.5 mL distilled water and then serial dilutions performed of different concentrations of 31.25–500 µg/mL. ABTS scavenging ability was expressed as half-maximal effective concentration (EC_{50} in µg/mL).

α-glucosidase inhibition assay

p-Nitrophenyl-α-D-glucopyranoside (p-NPG), yeast α-glucosidase, sodium carbonate and acarbose were purchased from Sigma Aldrich and the α-glucosidase inhibition assay was performed using the procedure as reported by (Poovitha and Parani 2016). Each sample was prepared by adding of 500 µl phosphate buffer (67mM, pH=6.9), 100 µl fruit extract/acarbose (0.25-4.0 mg/ml) with 100 µl of α-glucosidase (0.5 U/ml). The mixture was incubated at room temperature for 15 minutes. 250 µl of pNPG (50 mM in phosphate buffer) was used as substrate and then added to the sample and the mixture was re-incubated at room temperature. The reaction was stopped by using of 200 µl (0.1 M) sodium carbonate. The absorbance was measured at the wavelength of 405 nm using a spectrophotometer. Acarbose and distilled water were used as positive and negative controls, respectively. The percentage of α-glucosidase enzyme activity was calculated as follows:

$$\text{Inhibition of Sample (\%)} = [(A_0 - A_s)/A_0] \times 100$$

where A_0 is the absorbance of the control and A_s is the absorbance of the sample.

UPLC-ESI-MS experiments

For mass spectrometric detection, a high-resolution mass spectrometer (Waters Synapt G2-S) was used. The separation was analyzed using reverse phase chromatography on a Waters Acquity UPLC BEH C18 column (2.1 × 50 mm column size, 1.7 µm particle size). The system is equipped with a binary solvent (mobile phase), a column controller and sample chamber. The mobile phase solvent consisted of water containing 0.1% formic acid (elution buffer A) and acetonitrile containing 0.1% formic acid (elution buffer B). The initial conditions were 95% A at a flow rate of 0.2 mL/min. After that it was processed by multiple linear gradients to 5% A and then again to 95% A at 22 min. The polarity ES (in negative ionization mode) was used for mass analysis, with a mass range m/z between 50 to 1500. The optimal conditions for analysis were achieved with an injection volume of 10 µL, a capillary voltage of 2 kV, and sampling cone voltage of 40 eV. The source temperature was 150 ^{0}C and the desolvation temperature was set at 350 ^{0}C. The standard mass of Leucine Enkephalon (554.2615 Da in negative mode) was used as the reference for mass calibration. The spectra were processed and analyzed using Waters Masslynx^{TM} v4.1 software.

We performed targeted mass-spectrometric analysis of methanol extracts of different parts of the M. charantia fruit, in order to validate the presence of the steroids and phenolic compounds that were identified via NMR fingerprinting. These targeted metabolites underwent the same chromatographic conditions and were separated and eluted off the C18 column between 0 to 22 min. The identified metabolites present in the skin, pericarp and seed extracts based on the detection of $[M-H]^-$ ions are reported in Table S35 (supplementary material). The corresponding chromatogram and mass spectra of the plant extracts are given in Figures S24-27 (supplementary material). The values of the first three peaks to be identified were those of epicatechin, isorhamnetin and beta-sitosterol, corresponding to retention time R_t = 0.67 min and m/z values of 289, 315 and 413, respectively. The next peaks to be identified were those of catechin, syringic acid and stigmasterol at R_t = 5.909 min and m/z values of 289, 197 and 411, respectively.

References

Fan G, Luo WZ, Luo SH, Li Y, Meng XL, Zhou XD, Zhang Y. 2014. Metabolic discrimination of Swertia mussotii and Swertia chirayita known as “Zangyinchen” in traditional Tibetan medicine by ^{1}H NMR-based metabolomics,. J Pharm Biomed Anal. 98:364–370.

Sumner LW, Amberg A, Barrett D, Beale MH, Beger R, Daykin CA, Fan TWM, Fiehn O, Goodacre R, Griffin JL, et al. 2007. Proposed minimum reporting standards for chemical analysis. Metabolomics. 3(3):211–221.

Savorani F, Tomasi G, Engelsen S. 2010. icoshift: A versatile tool for the rapid alignment of 1D NMR spectra. J Magn. 202(2):190 – 202.

Gogna N, Hamid N, Dorai K. 2015. Metabolomic profiling of the phytomedicinal constituents of carica papaya L. leaves and seeds by ^{1}H NMR spectroscopy and multivariate statistical analysis. J Pharm Biomed Anal. 115:74.

Zhou K, Wang H, Mei W, Li X, Luo Y, Dai H. 2011. Antioxidant activity of papaya seed extracts. Molecules. 16(8):6179–6192.

Meda A, Lamien CE, Romito M, Millogo J, Nacoulma OG. 2005. Determination of the total phenolic, flavonoid and proline contents in burkina fasan honey, as well as their radical scavenging activity. Food Chem. 91(3):571–577.

Rajurkar NS, Hande SM. 2011. Estimation of phytochemical content and antioxidant activity of some selected traditional indian medicinal plants. Indian J Pharm Sci. 73(2):146.

Poovitha S, Parani M. 2016. In vitro and in vivo α-amylase and α-glucosidase inhibiting activities of the protein extracts from two varieties of bitter gourd (Momordica charantia L.). BMC Complement Altern Med. 16(1):185.

Supplementary Figures and Tables

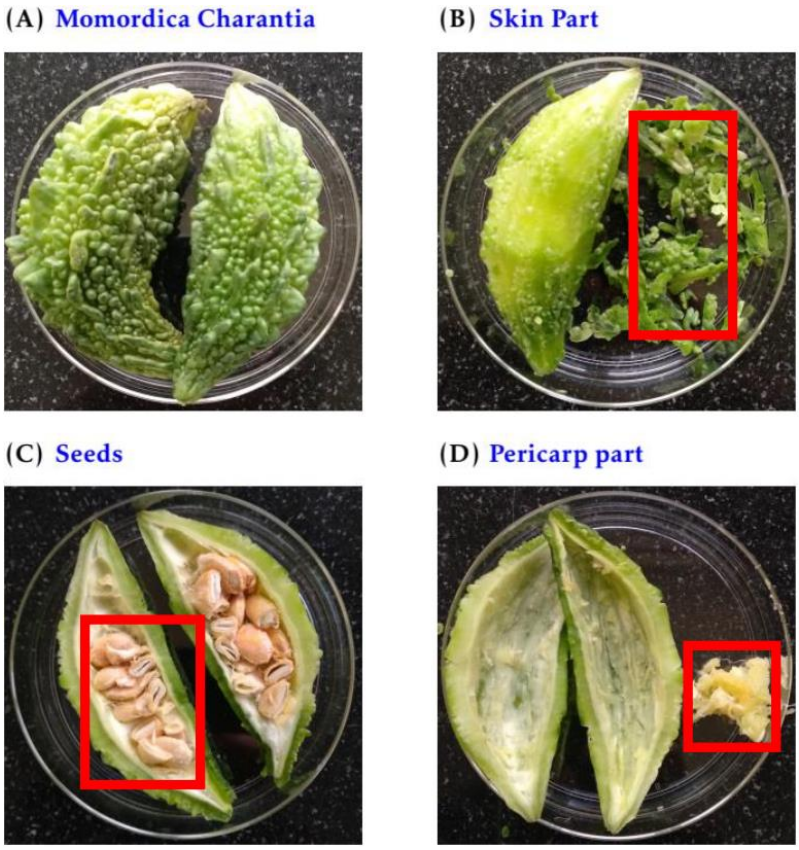

Figure S1: Different parts of M. charantia. (A) Fruit, (B) Removal of skin part, (C) Mature seeds, and (D) Removal of pericarp inside of the fruit.

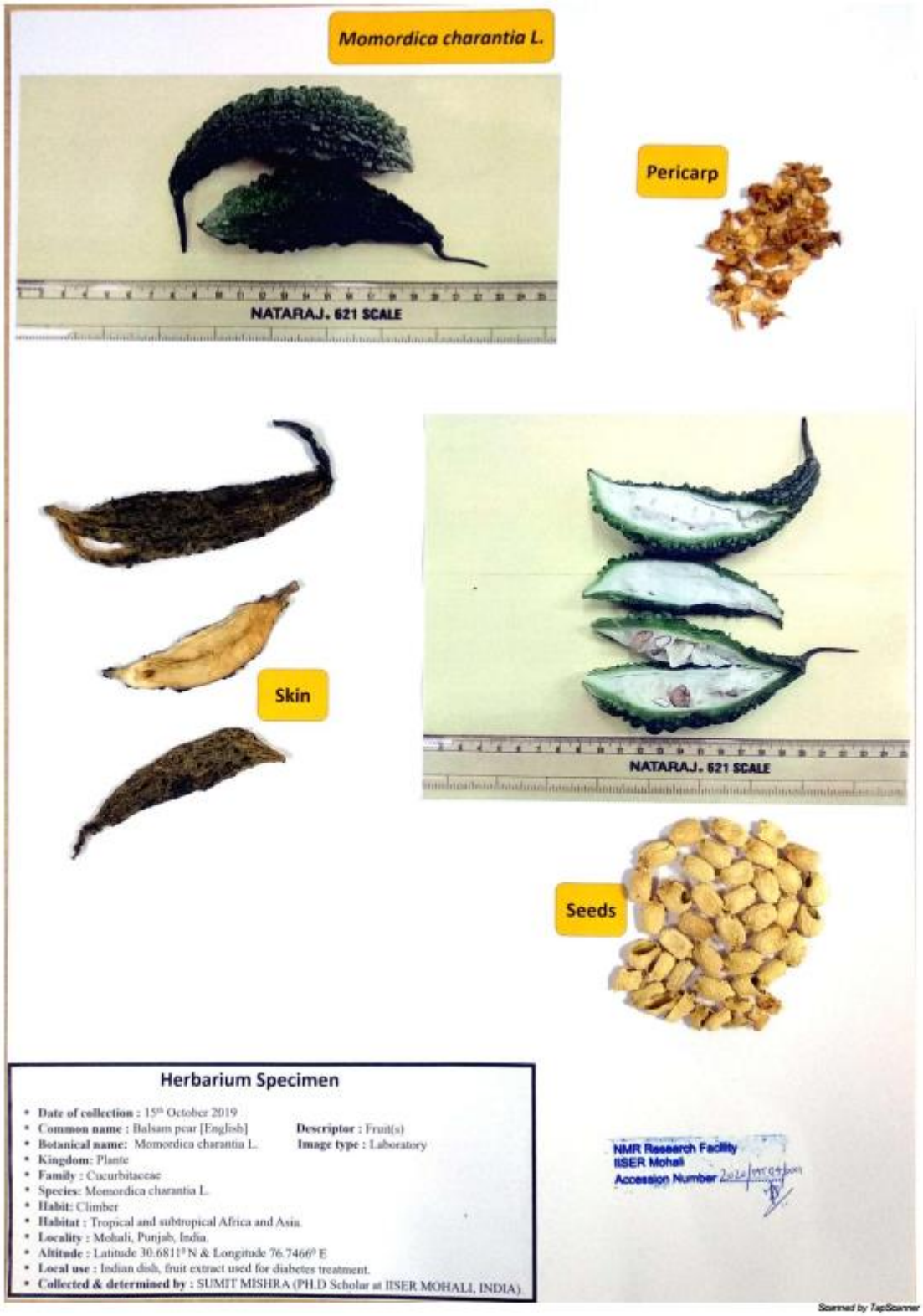

Figure S2: Voucher specimen was deposited at the NMR research facility IISER Mohali (Voucher accession number.: 2020/MT04/0001).

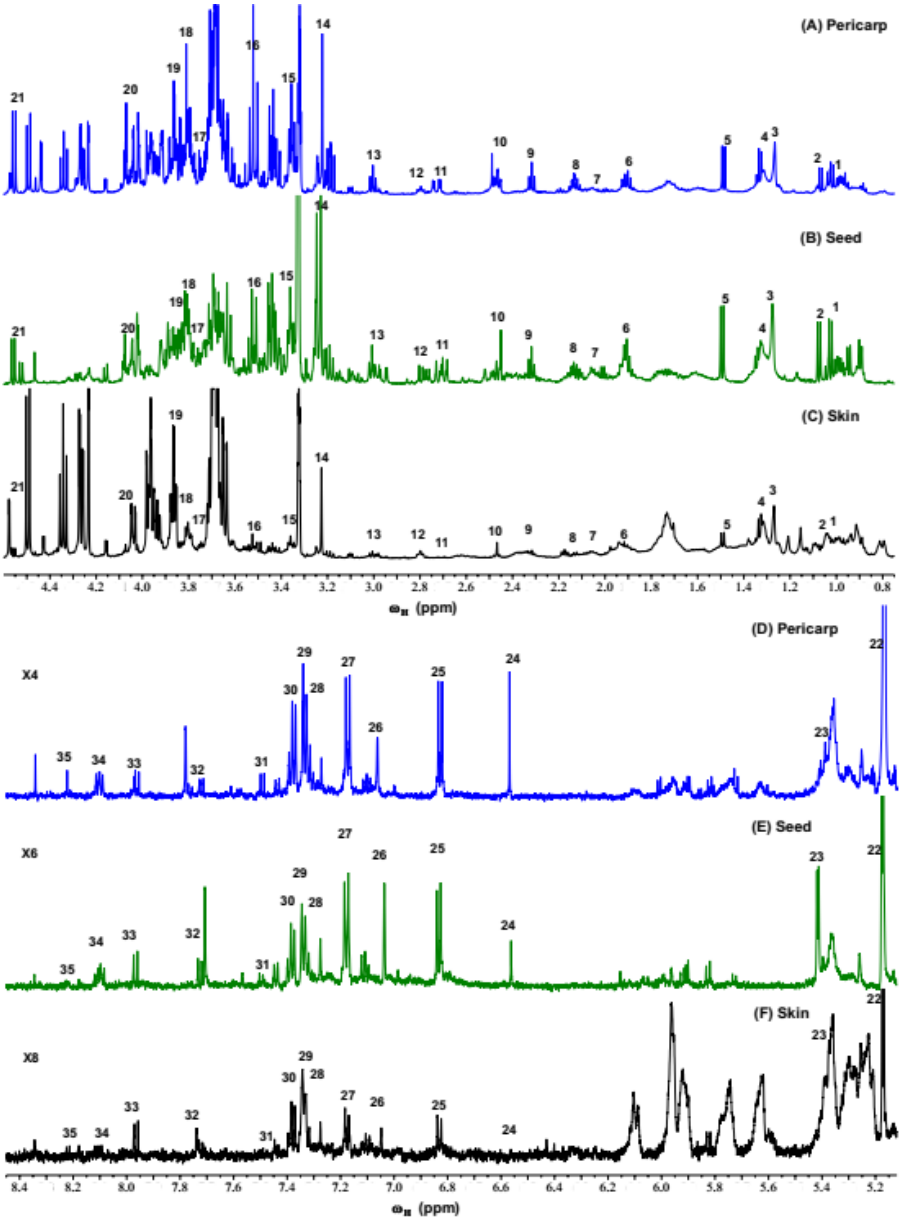

Figure S3: Representative ^{1}H NMR spectrum of M. charantia extracts: (A) & (D) pericarp, (B) & (E) seed and (C) & (F) skin, recorded at 600 MHz, showing identified metabolites. Peak labeling: 1, charantin; 2, valine; 3, lipid(-CH_2)n; 4, lactic acid; 5, alanine; 6, leucine; 7, chlorogenic acid; 8, glutamine/glutamic acid; 9, gamma- Aminobutyric acid (GABA); 10, epicatechin; 11, malic acid; 12, aspartic acid; 13, lysine; 14, choline; 15, inositol; 16, glycine; 17, arginine; 18, syringic acid; 19, threonine; 20, proline; 21, catechin; 22, alpha-glucose; 23, sucrose; 24, luteolin; 25, gentisic acid; 26, gallic acid; 27, tyrosine; 28, naringenin; 29, myricetin; 30, protocatechuic acid; 31, tryptophan; 32, trans-Cinnamic acid; 33, daidzein; 34, kaempferol; 35, adenine.

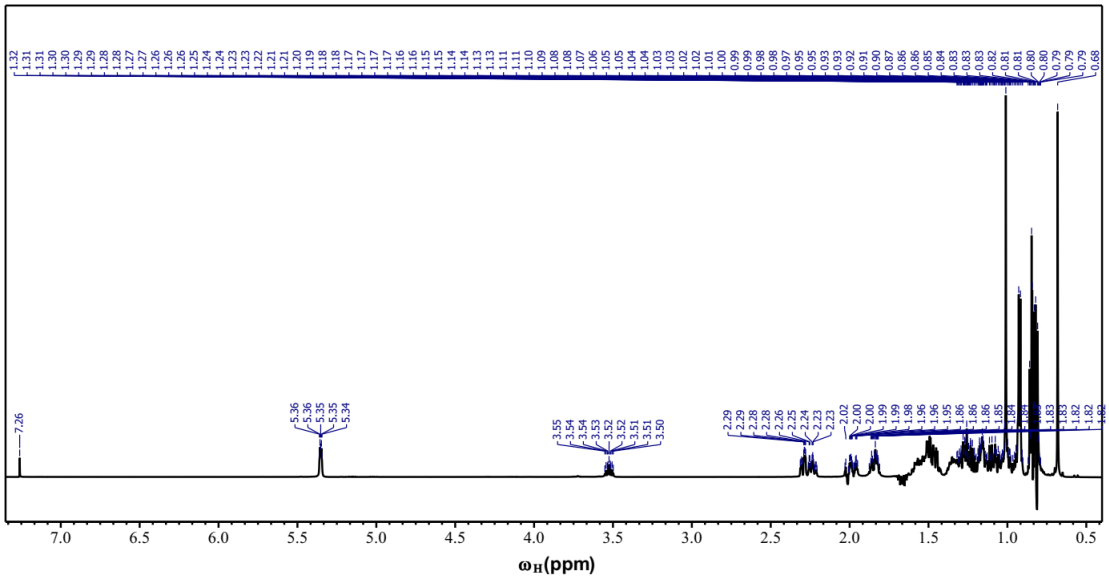

Figure S4: 1D ^{1}H NMR spectra of beta-sitosterol recorded at 600 MHz spectrometer.

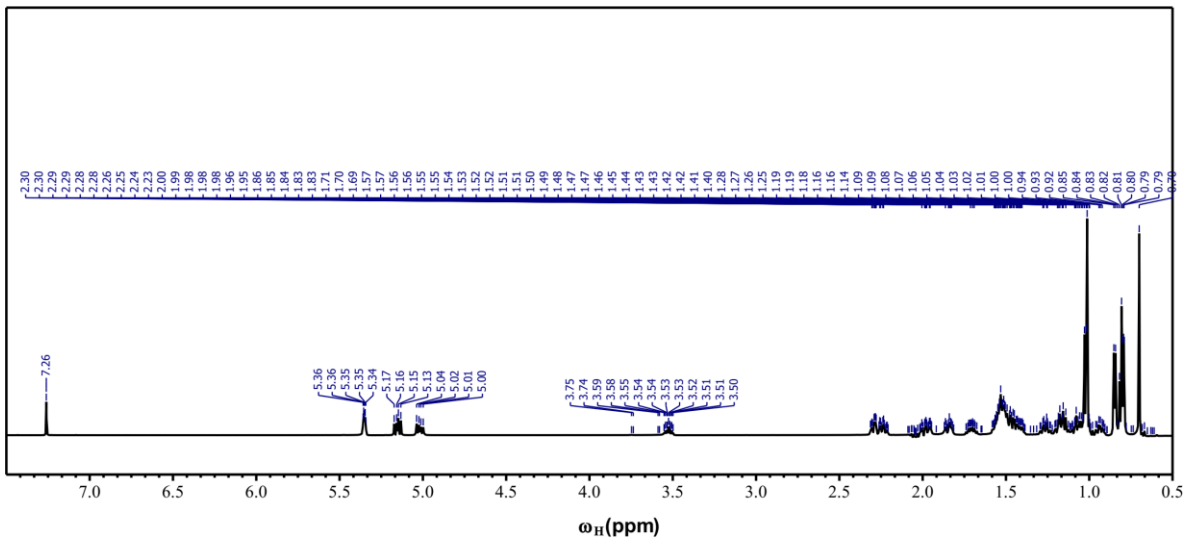

Figure S5: 1D ^{1}H NMR spectra of stigmasterol recorded at 600 MHz spectrometer.

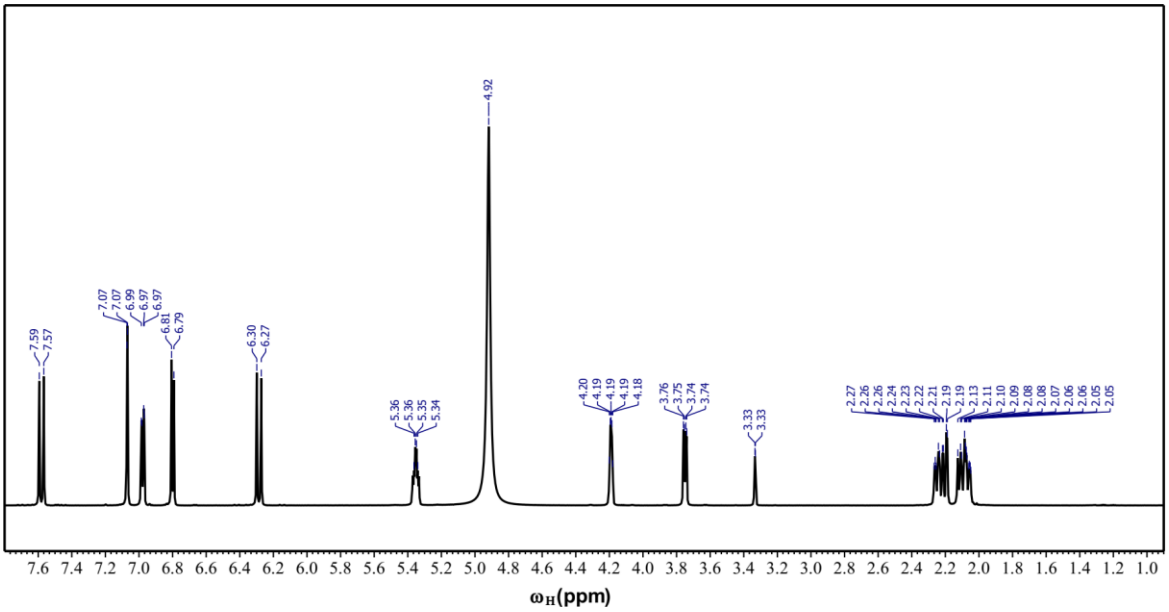

Figure S6: 1D ^{1}H NMR spectra of chlorogenic acid recorded at 600 MHz spectrometer.

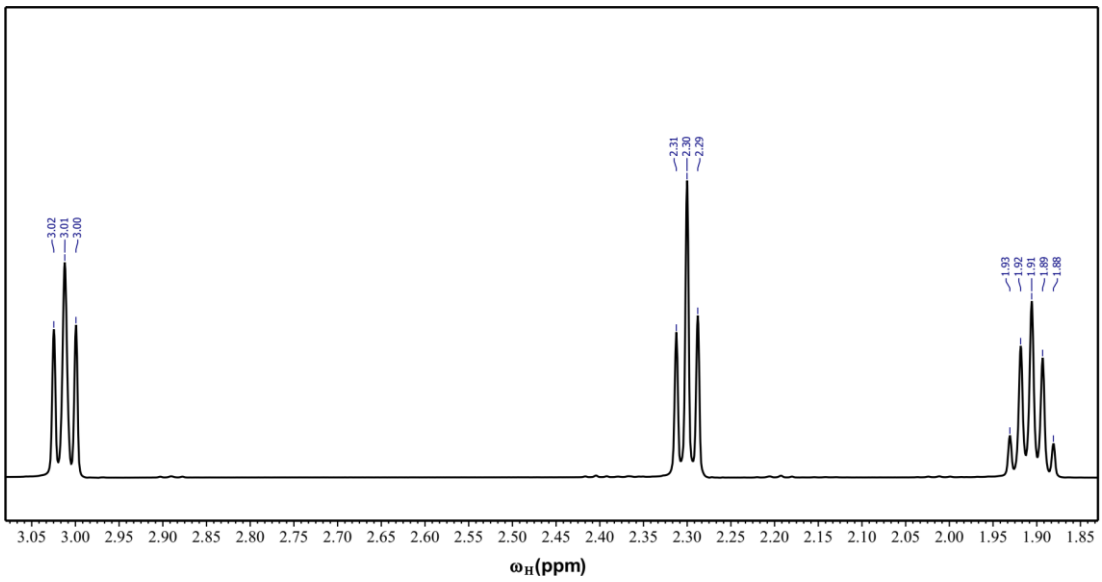

Figure S7: 1D ^{1}H NMR spectra of gamma-Aminobutyric acid recorded at 600 MHz spectrometer.

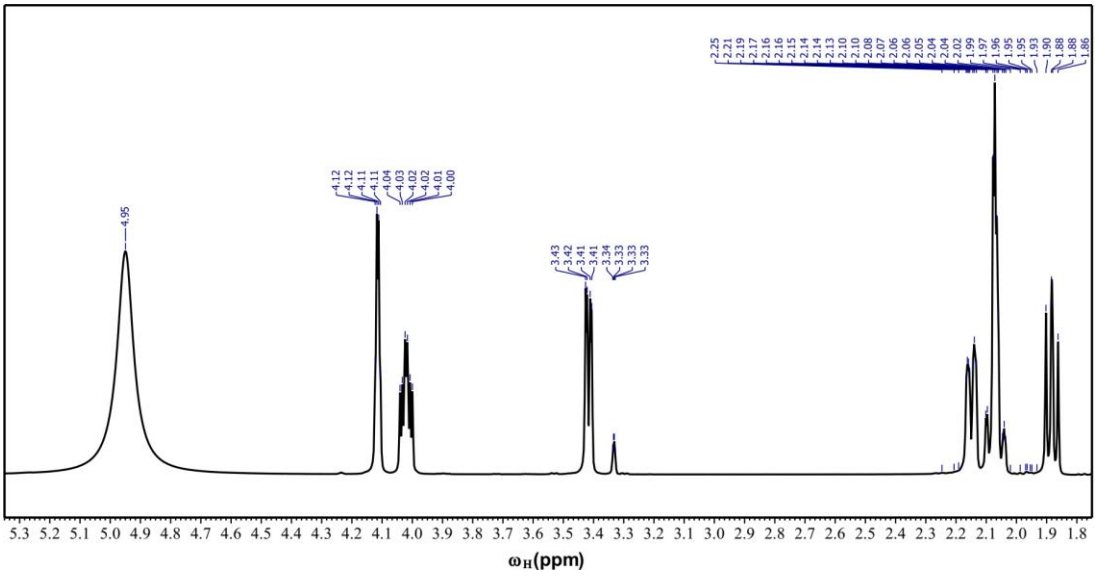

Figure S8: 1D ^{1}H NMR spectra of quinic acid recorded at 600 MHz spectrometer.

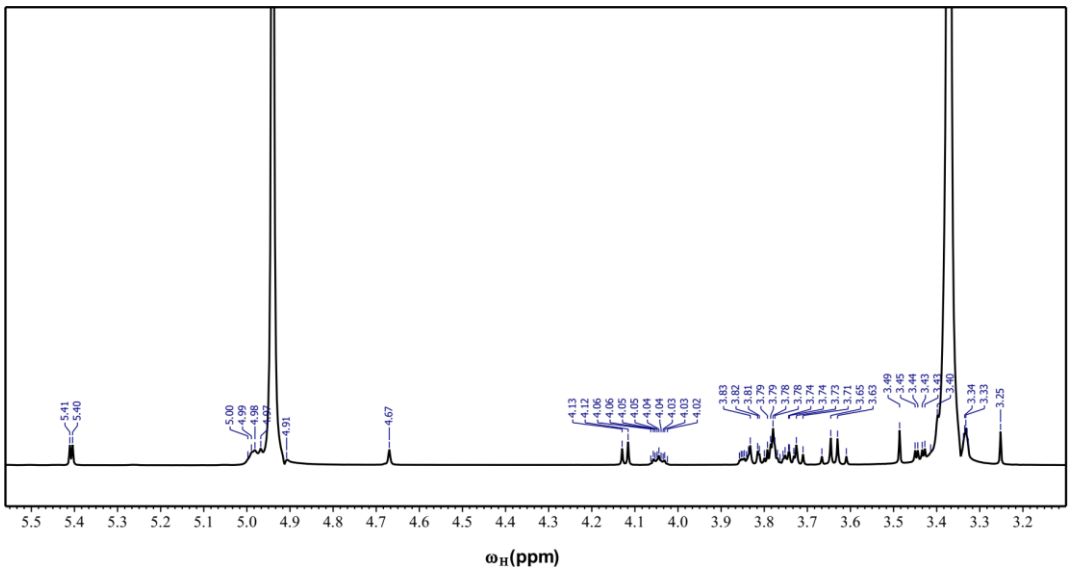

Figure S9: 1D ^{1}H NMR spectra of sucrose recorded at 600 MHz spectrometer.

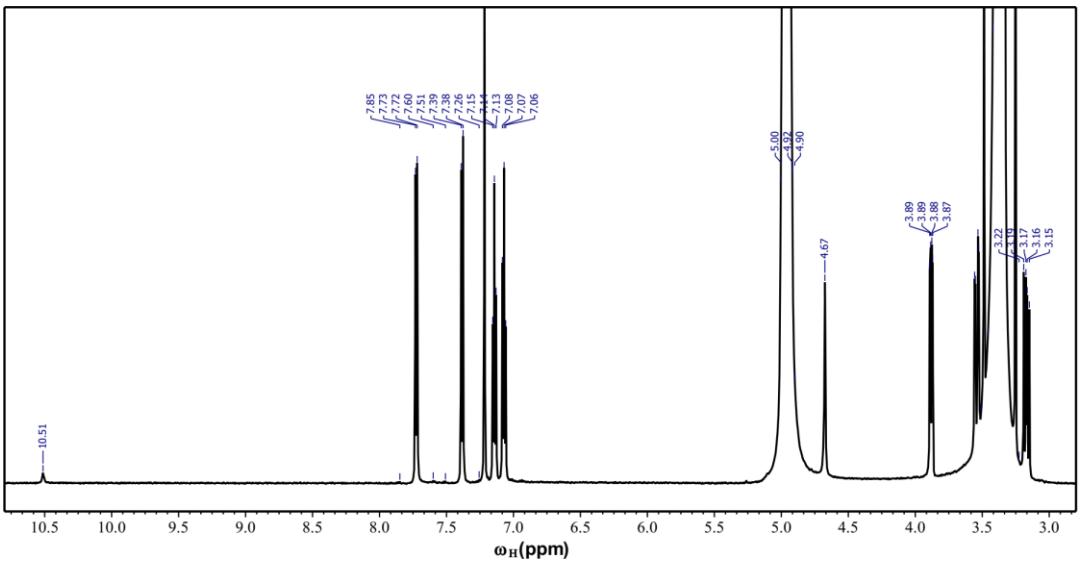

Figure S10: 1D ^{1}H NMR spectra of tryptophan recorded at 600 MHz spectrometer.

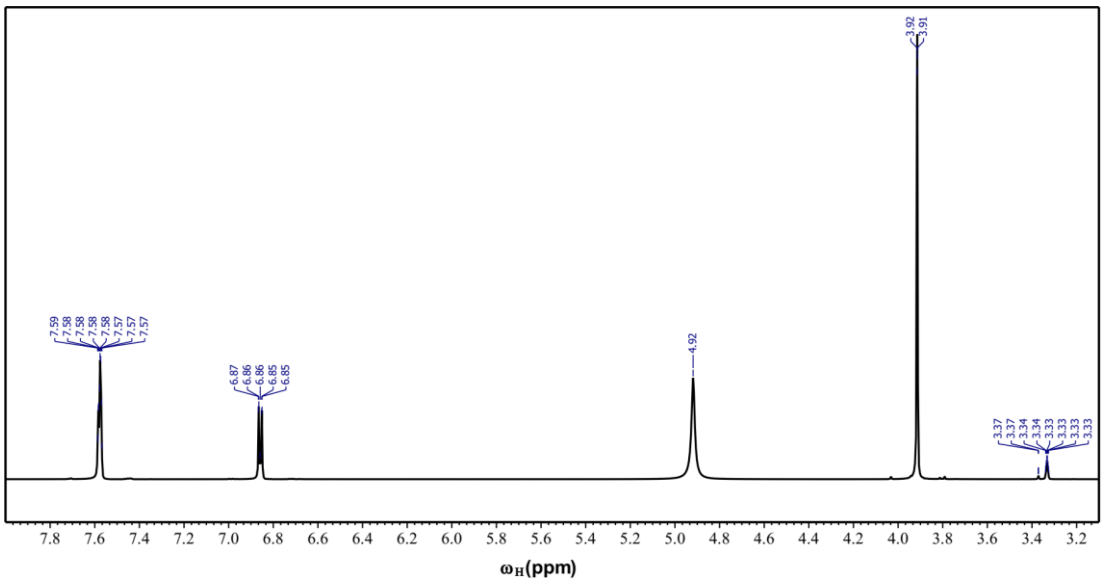

Figure S11: 1D ^{1}H NMR spectra of vanillic acid recorded at 600 MHz spectrometer.

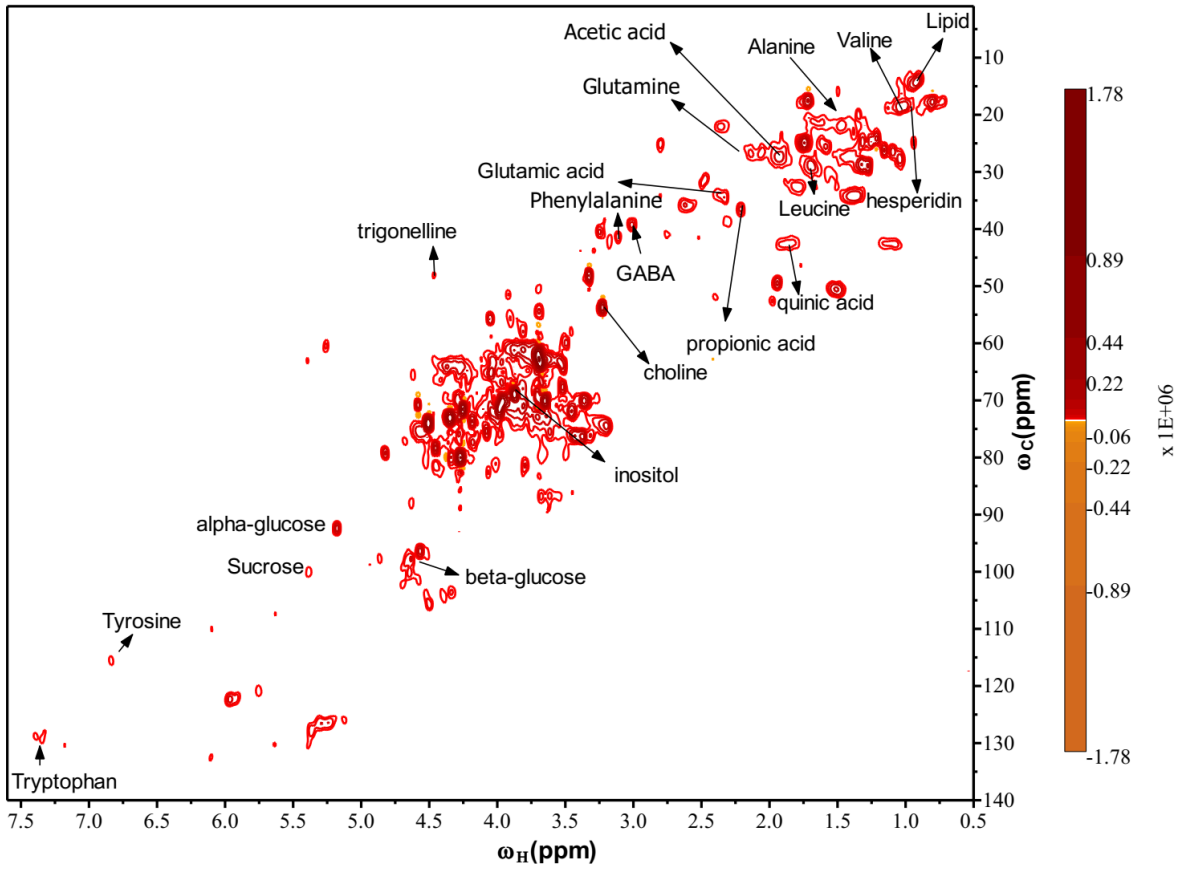

Figure S12: 2D ^{1}H-^{13}C HSQC NMR spectrum of M. charantia skin, recorded at 600 MHz. Proton chemical shift (ω_H ppm) is represented along X-axis and carbon chemical shift (ω_C ppm) is represented along Y-axis. Spectra recorded with J value = 145.

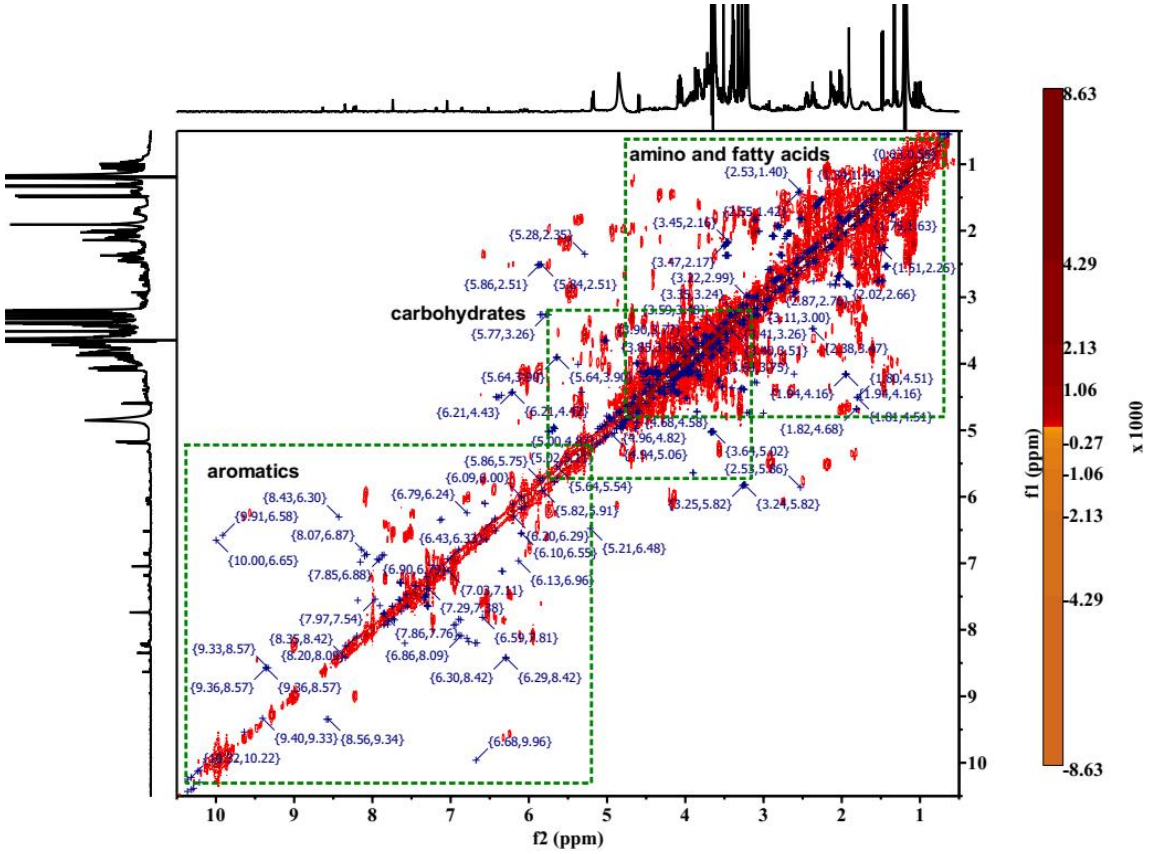

Figure S13: ^{1}H-^{1}H COSY NMR spectrum of M. charantia skin extract recorded at 600 MHz showing amino acid, lipids, carbohydrates and aromatics peaks. Proton chemical shifts (ω_H ppm) are represented along both spectral dimensions.

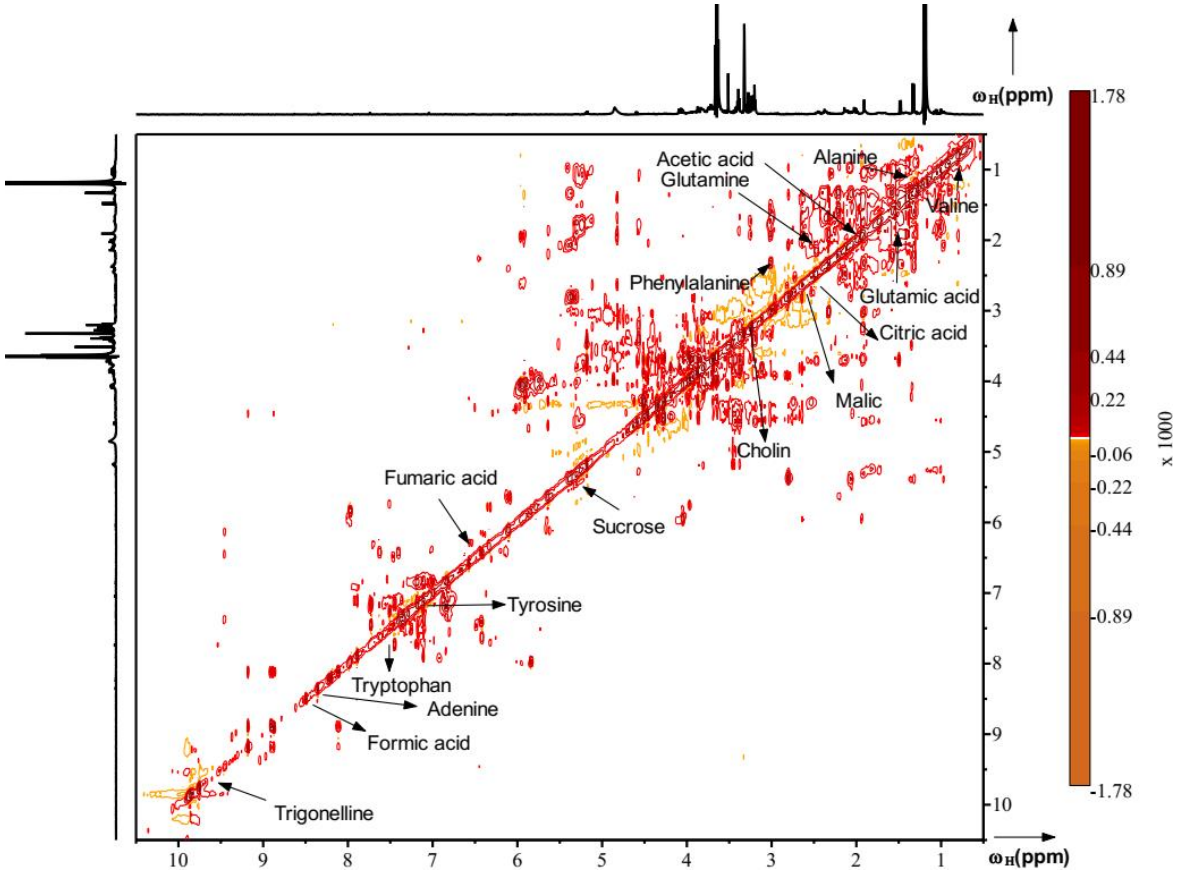

Figure S14: The two-dimensional TOCSY spectra of M. charantia skin extract in the region of δ 0.5 to 10.5 showing amino acid, lipids, carbohydrate and aromatic peaks.

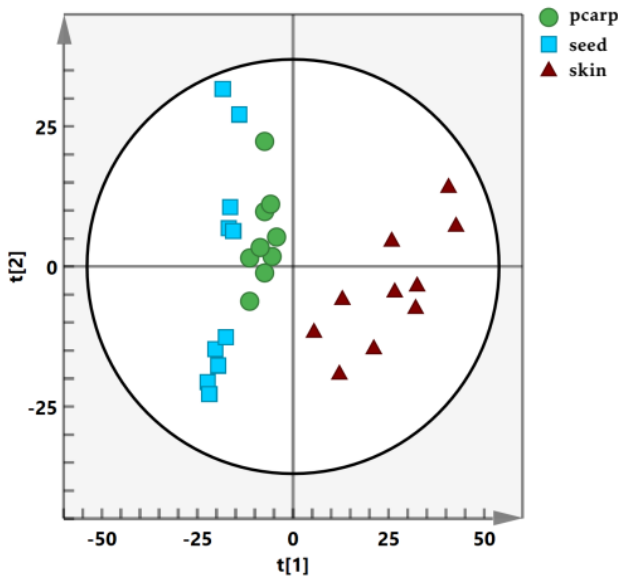

Figure S15: Principal component analysis (PCA) score plot of pcarp (pericarp), seed and skin part of M. charantia with component 1 explaining 70.1 % of the variation and component 2 explaining 16.6 % of the variation, showing a clear separation between these three groups.

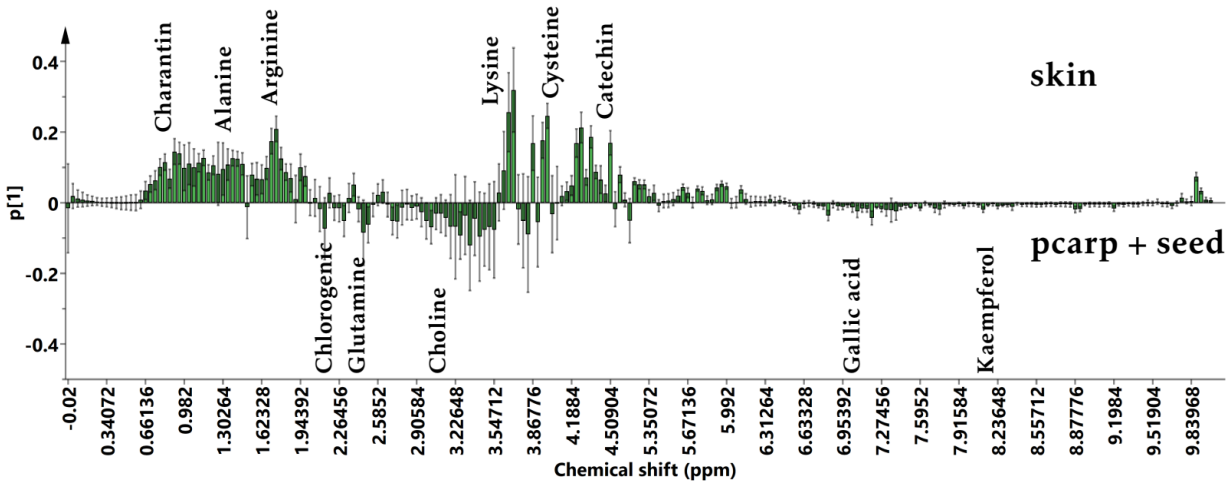

Figure S16: PCA column loading plot represent significant differences: The concentration of the following compounds charantin, alanine, arginine, lysine, cysteine and catechin are found to be more in skin part of M. charantia. While chlorogenic acid, glutamine, choline, gallic acid and kaempferol are showing high concentration in pcarp + seed part of the fruit.

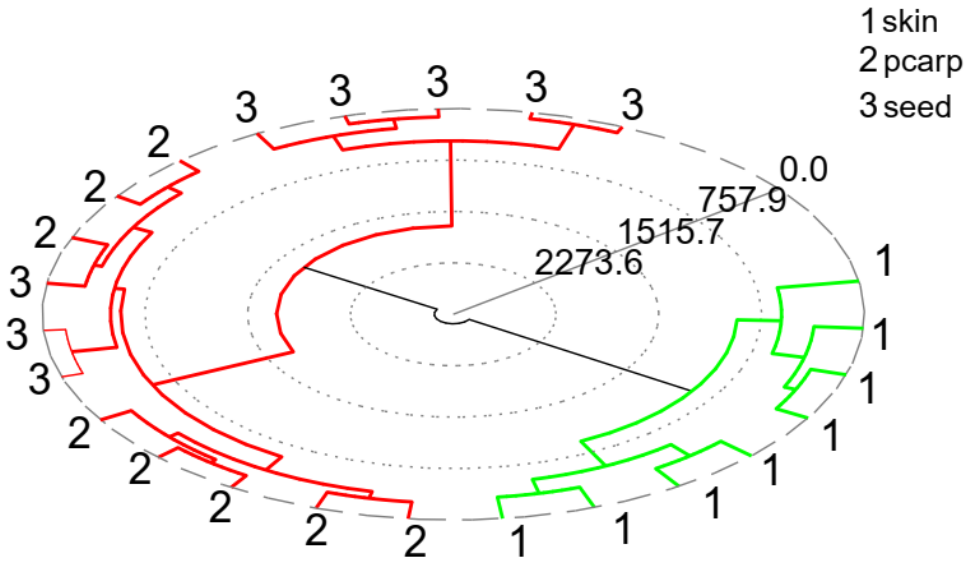

Figure S17: The polar dendrogram illustrates hierarchical clustering between all the three parts of M. charantia. Labellings are as follows: 1-Skin; 2-pcarp (pericarp); 3-seed.

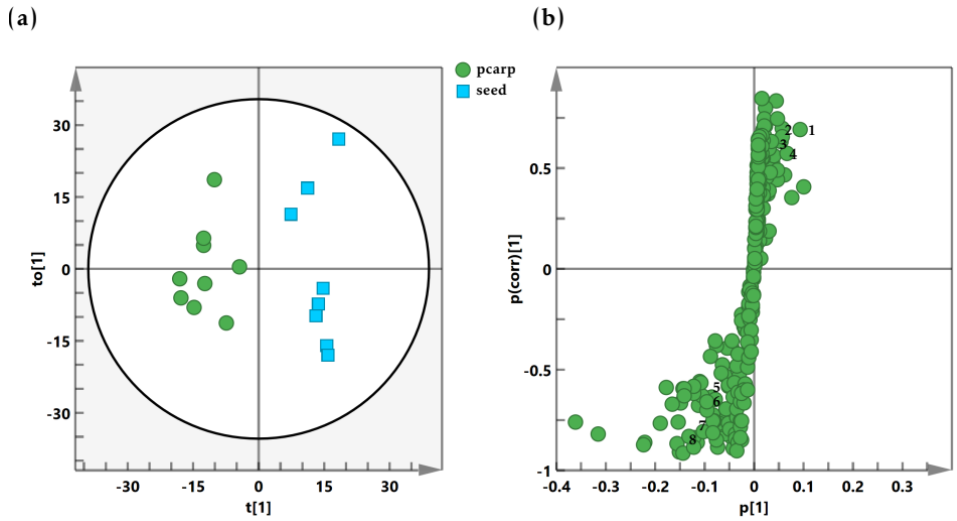

Figure S18: (a) OPLS-DA score plot obtained from 1D ^{1}H NMR spectra of seed and pcarp (pericarp). (b) S plot showing the metabolites responsible for the discrimination between the groups. Cutoff values for the covariance of $|p[1]| \geq 0.05$ and for the correlation of $|p(corr)[1]| \geq 0.5$ were used. The labels correspond to: 1, choline; 2, epicatechin; 3, phenylalanine; 4, lysine; 5, lactic acid; 6, methyl group $(-CH_2)n$; 7, alpha-glucose; 8, beta-glucose.

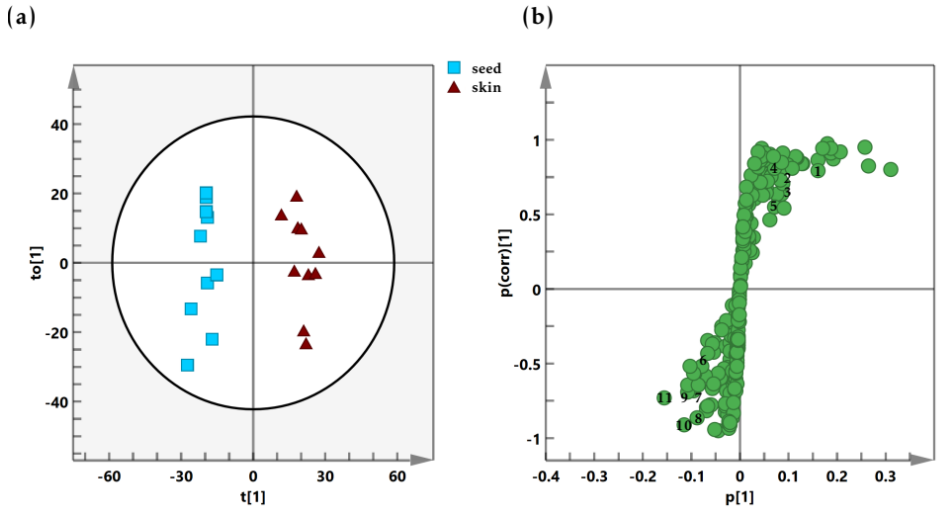

Figure S19: (a) OPLS-DA score plot obtained from 1D ^{1}H NMR spectra of seed and skin. (b) S plot showing the metabolites responsible for the discrimination between the groups. Cutoff values for the covariance of $|p[1]| \geq 0.05$ and for the correlation of $|p(corr)[1]| \geq 0.5$ were used. The labels correspond to: 1, threonine; 2, lactic acid; 3, charantin; 4, sucrose; 5, $(-CH_2)n$; 6, glycine; 7, glutamine; 8, lysine; 9, epicatechin; 10, choline; 11, inositol.

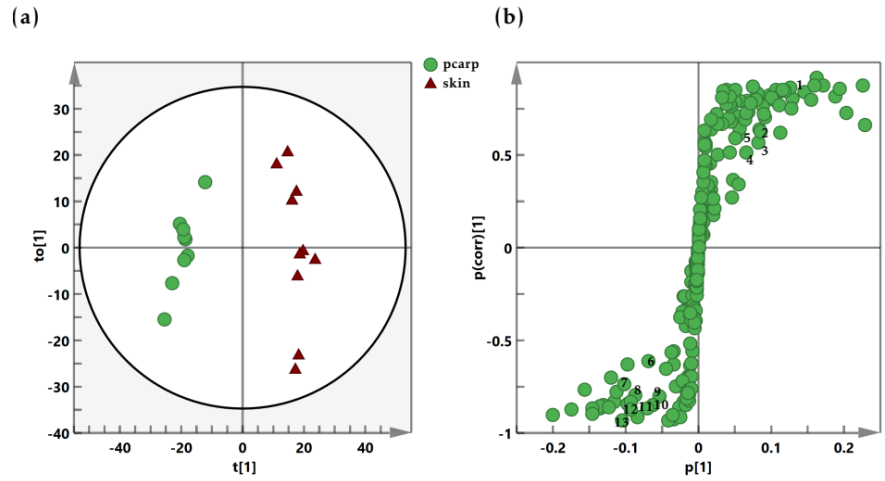

Figure S20: (a) OPLS-DA score plot obtained from 1D ^{1}H NMR spectra of skin and pcarp (pericarp). (b) S plot showing the metabolites responsible for the discrimination between the groups. The labels correspond to: 1, lipid methyl group $(-CH_2)n$; 2, lactic acid; 3, charantin; 4, lipid methyl group; 5, catechin; 6, proline; 7, arginine; 8, glutamic acid; 9, GABA; 10, malic acid; 11, lysine; 12, beta-glucose; 13, alpha-glucose.

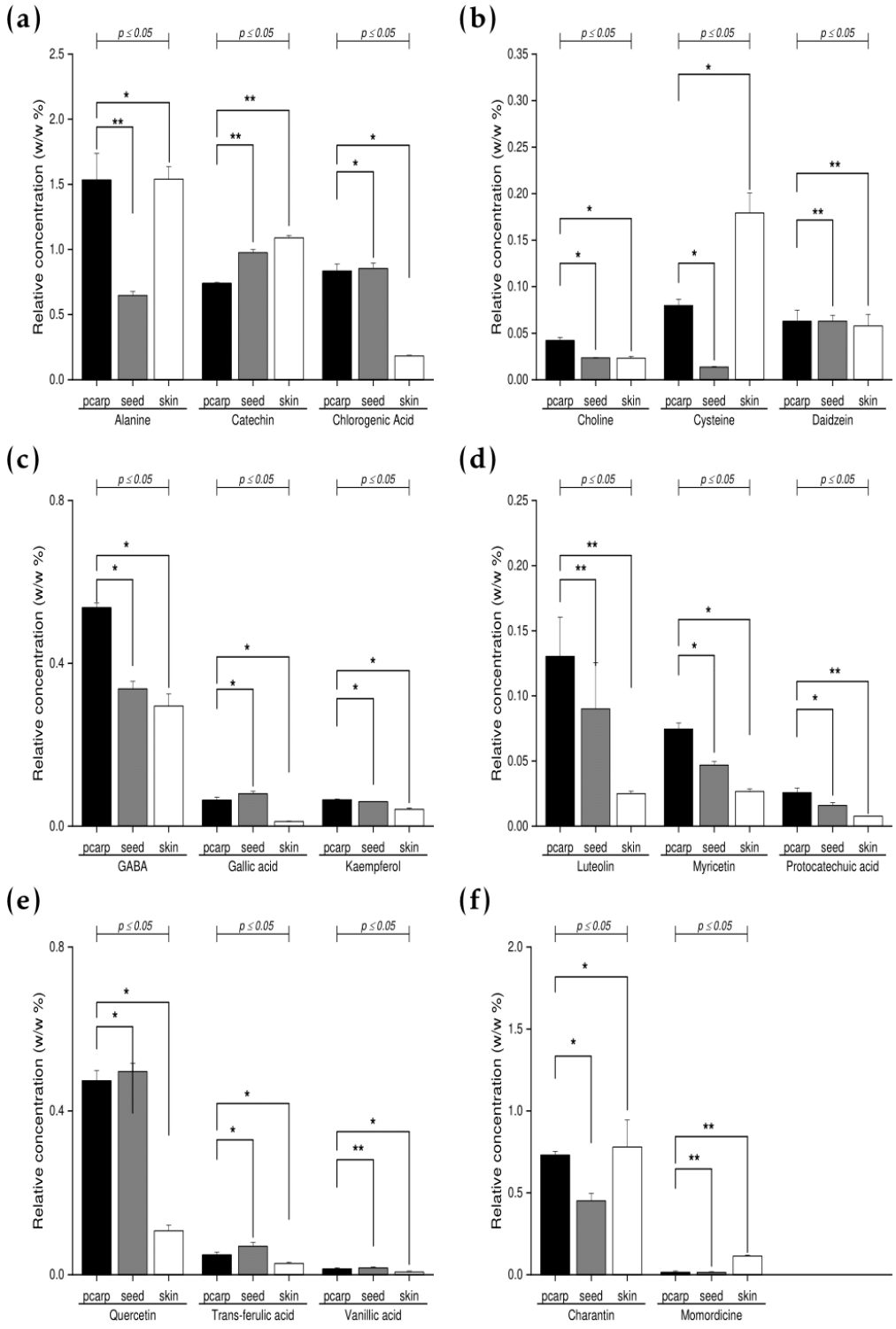

Figure S21: Relative concentrations (w/w %) of significantly different metabolites in M. charantin extracts (pericarp, skin and seed) as detected by ^{1}H NMR experiments. The label $*$ indicates a significant metabolite ($p \leq 0{:}05$), while the metabolites marked with $**$ are not significant.

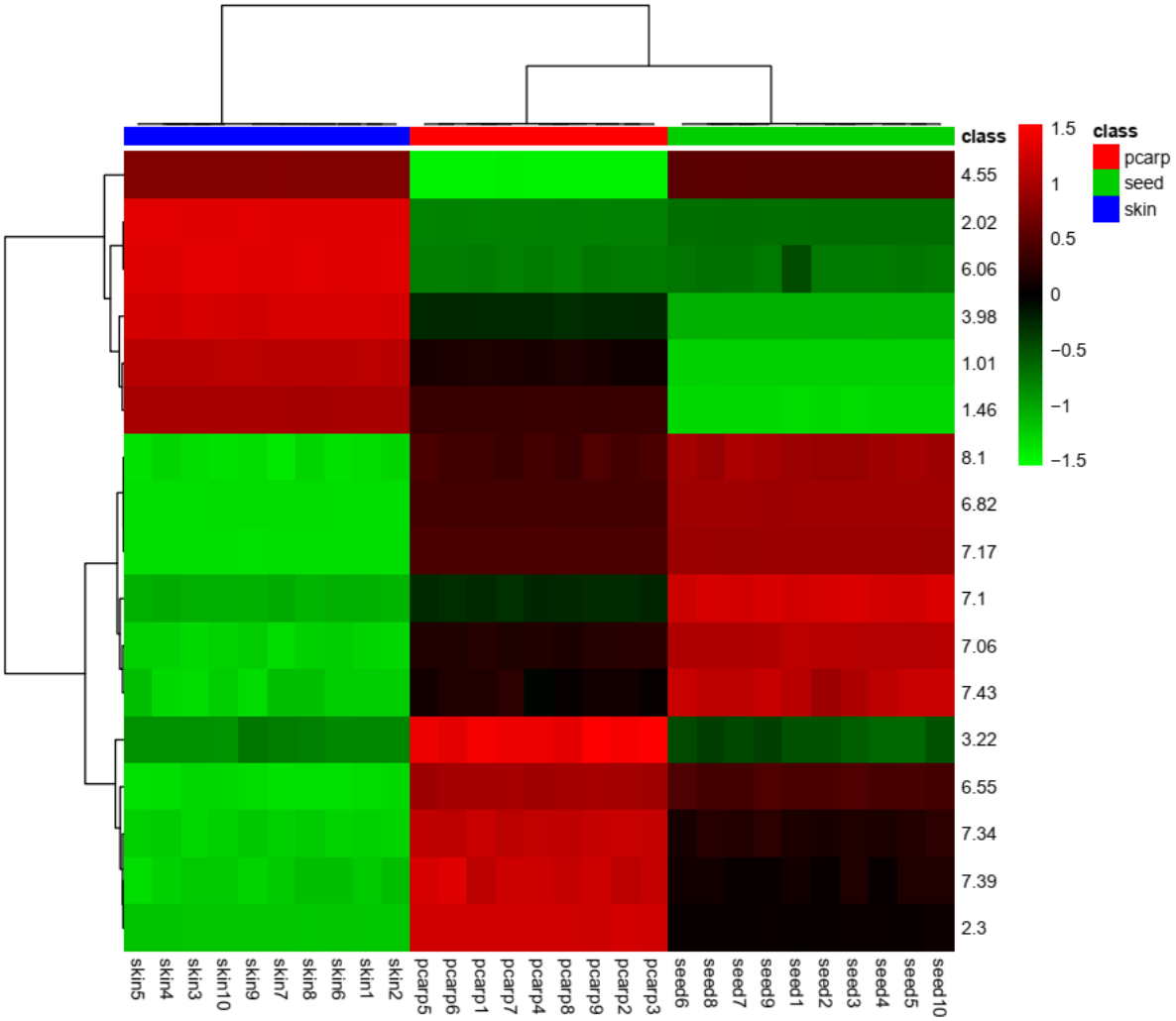

Figure S22: Dendrogram and heat map generated by hierarchical cluster analysis for significant metabolites identified from different parts of M. charantia (Rows: groups and Columns: metabolites). The two groups pericarp and seed were clustered together and are separated by the third group skin. Positive (red) or negative (green) correlations denote a increase or decrease in the metabolite concentrations, respectively. The hierarchical tree was constructed using Ward's minimum variance and Euclidean distance metric. The dendrogram is shown on the top of the heat map (pericarp-(red), seed-(green), skin-(blue)) and unveils the connection between the different groups based on their metabolite abundance levels.

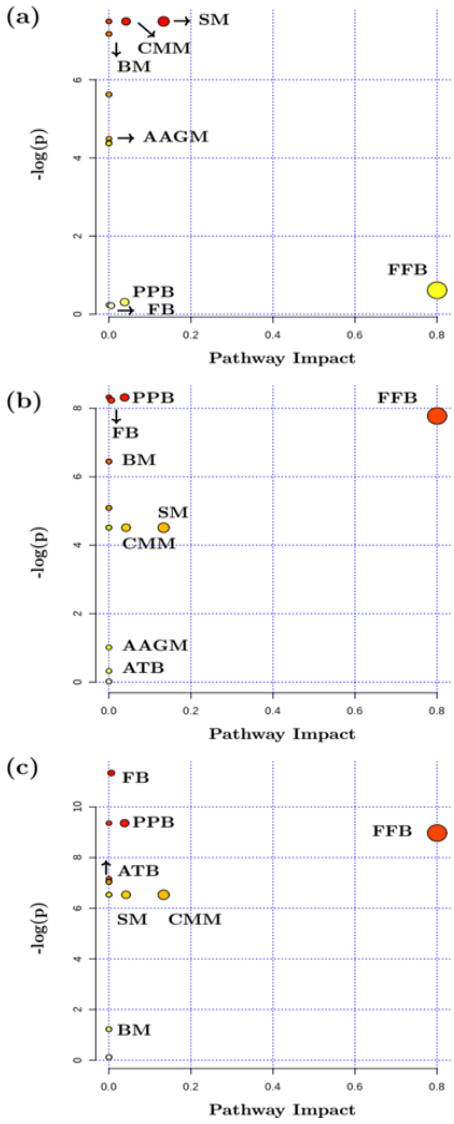

Figure S23: Metabolic pathway impact analysis was performed via MetaboAnalyst (MetPa) for (a) Pericarp and seed, (b) Pericarp and skin, (c) Skin and seed, showing the significant changes in all the groups. FB: Flavonoid biosynthesis, PPB: Phenylpropanoid biosynthesis, ATB: Aminoacyl-tRNA biosynthesis, SM: Sulfur metabolism, FFB: Flavone and flavonol biosynthesis, CMM: Cysteine and methionine metabolism, BM: Butanoate metabolism, AAGM: Alanine, aspartate and glutamate metabolism. The compound colors of each circle are based on p-values while the size of the circle gives an idea of the impact value within the metabolome pathway (larger circles imply greater impact). The yellow to red color range denotes different significance levels of the metabolites.

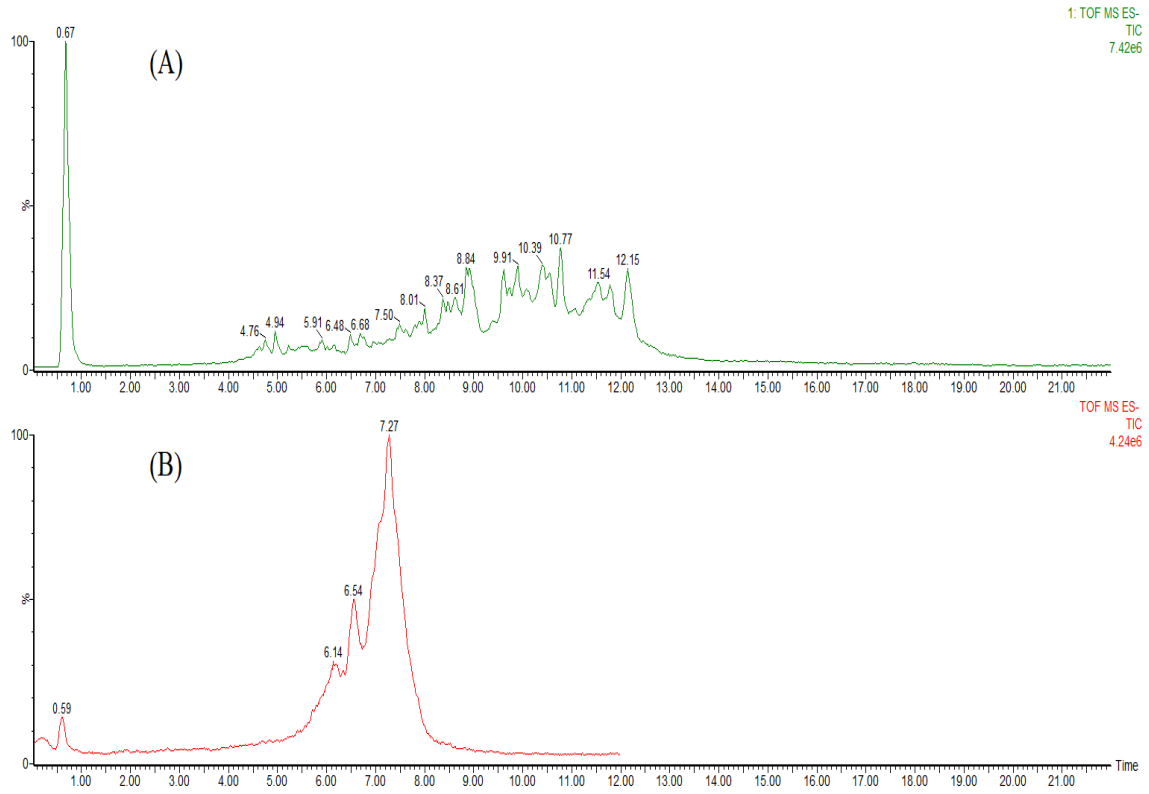

Figure S24: UPLC-MS chromatogram (A) shows the of M. charantia skin sample, whereas (B) shows the blank sample. These samples run in negative ESI mode.

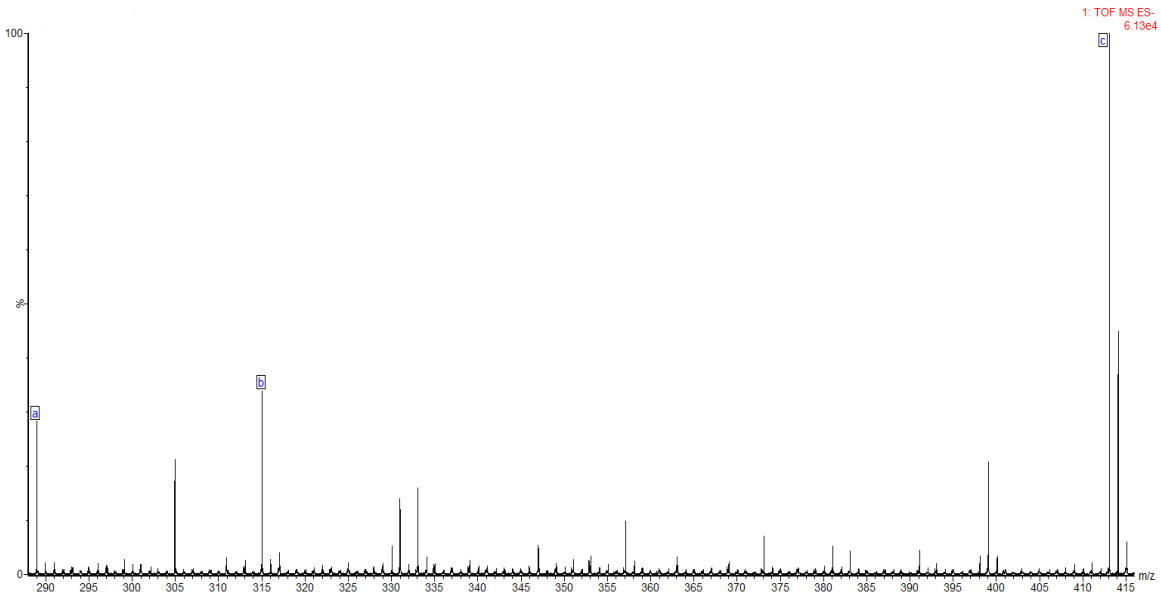

Figure S25: Mass spectra showing the detected metabolites masses $[M-H]^-$ ions: (a); epicatechin, (b); isorhamnetin and (c); beta-sitosterol.

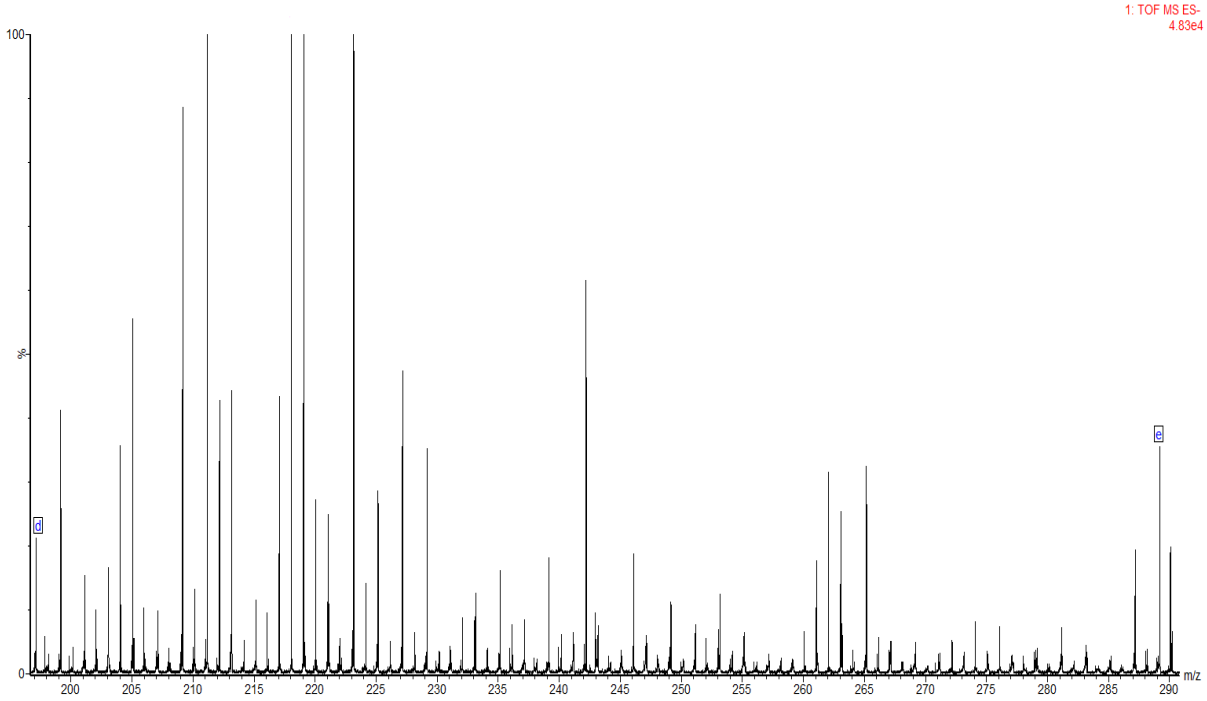

Figure S26: Mass spectra showing the detected metabolites masses $[M-H]^-$ ions: (d); catechin, and (e); syringic acid.

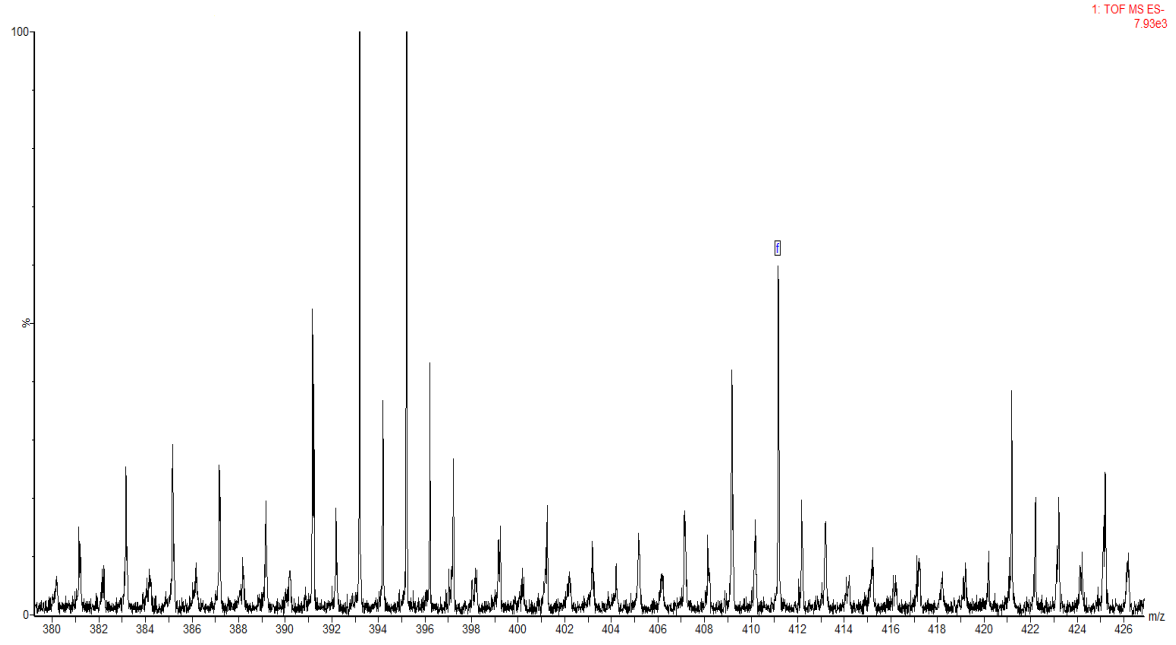

Figure S27: Mass spectra showing the detected metabolite mass $[M-H]^-$ ion: (f); stigmasterol.

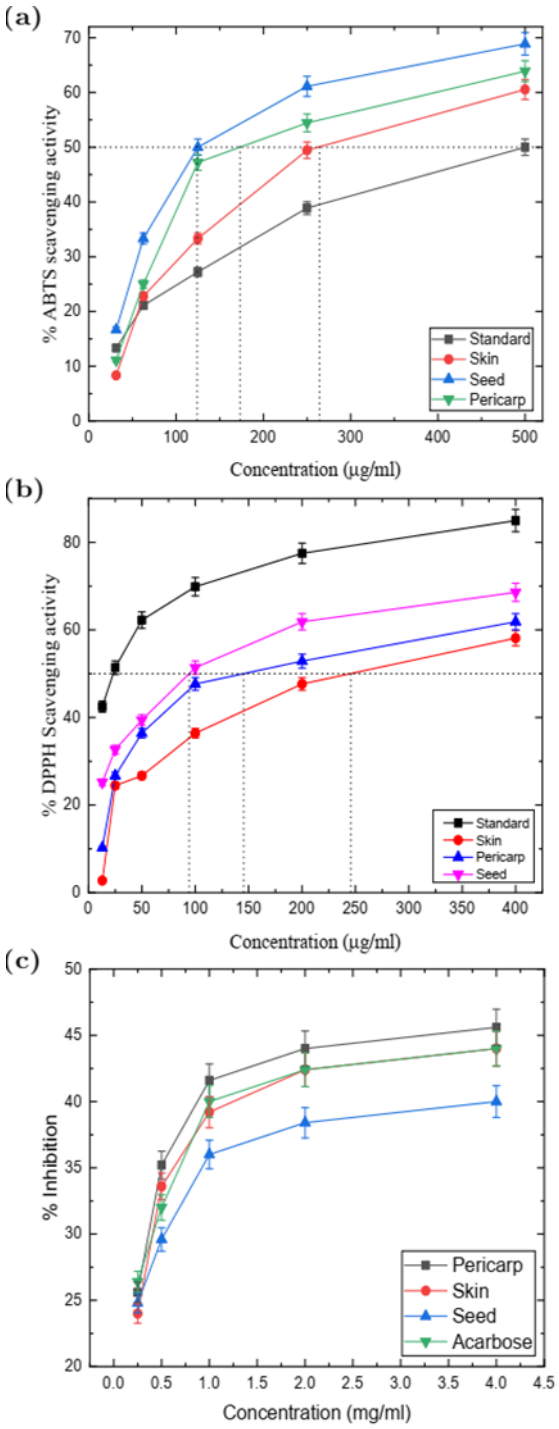

Figure S28: (a) Antioxidant potential of different parts of M. charantia (seed, pericarp and skin) from ABTS assay and using Trolox as a positive control. (b) Scavenging activity (%) of M. charantia extracts (seed, pericarp and skin) on DPPH radicals. (c) The percentage inhibition α-glucosidase activity of M. charantia extracts (pericarp, skin, seed) and acarbose (an anti-diabetic drug).

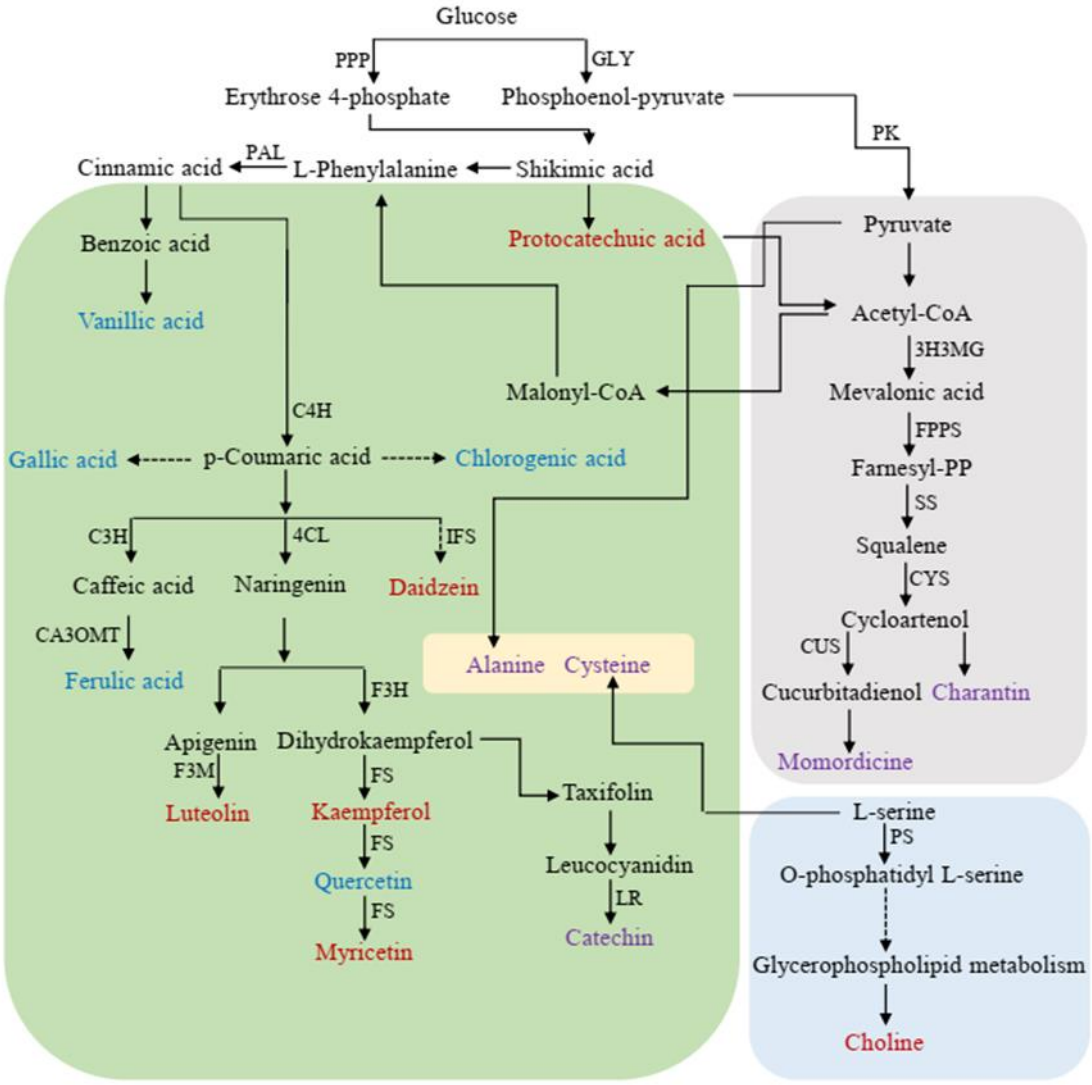

Figure S29: Metabolic pathway depicting the synthesis of significant secondary metabolites and linkage between them, identified via 600 MHz ^{1}H NMR experiments. Red, blue and purple colors indicate metabolites that are higher in concentration in pericarp, seed and skin respectively. Reactions considered are: GLY: glycolysis; PK: pyruvate kinase; PPP: pentose phosphate pathway; PAL: phenylalanine ammonia-lyase; C4H: cinnamate 4-hydroxylase; C3H: coumarate 3-hydroxylase; CA3OMT: caffic acid 3-O-methyltransferase; 4CL: 4-coumaroyl-CoA ligage; IFS: isoflavone synthase; F3H: flavanone 3-hydroxylase; F3M: flavonoid-3'-monooxygenase; FS: flavonol synthase; LR: leucocyanidin reductase; 3H3MG: 3-hydroxy-3-methyl-glutyrl-CoA reductase; FPPS: farnesyl PP synthase; SS: squalene synthase; CYS: cycloartenol synthase; CUS: cucurbitadienol synthase; PS: phosphatidylserine synthase.

Table S30: Primary plant metabolites identified from ^{1}H NMR and 2D NMR spectra of M. charantia, with chemical shifts in ppm and the corresponding multiplicity m and scalar coupling J values (in Hz).

Metabolites	**Chemical Shift (*m; J*)**	**Identification MSI**
Lipids		
Term. methyl group	0.86(t,6.95), 0.95(t,6.9)	Level 2
$(CH_2)n$	1.27(m)	Level 2
$CH_2CH_2COOH(C_3)$	1.64(m)	Level 2
CH_2COOH (C_2)	2.37(t,7.5)	Level 2
Allylic protons of unsaturated fatty acids	2.03(m)	Level 2
Olefinic proton of unsaturated fatty acids	5.3(m)	Level 2
Amino acids		
Leucine	0.95(t,6), 1.9(m)	Level 2
Valine	0.98(d,7), 1.06 (d,7), 2.29(m)	Level 2
Alanine	1.49 (d,7.3), 3.77(q,7.2)	Level 2
Glutamine	2.15(m), 2.47(m)	Level 2
Glutamic acid	2.15(m), 2.44(m)	Level 2
Phenylalanine	3.0(m), 7.32(d,6.9)	Level 2
Tyrosine	6.86(m), 7.19(m)	Level 2
Tryptophan	7.32(s), 7.54(d,7.54)	Level 1
GABA	1.90(m), 2.30(t,7.2),	Level 1
Aspartic acid	2.79(dd,17.6), 3.88(dd,8.5)	Level 2
Threonine	3.82(dd,5.74)	Level 2
Glycine	3.52(s)	Level 2
Methionine	2.62(t,7.49), 2.13(m)	Level 2
Isoleucine	1.01(d,7.01), 0.96(t,7.62)	Level 2
Histidine	3.19(dd,14.5), 7.77(d,1.04)	Level 2
Lysine	3.02(t), 3.74(t,6.09)	Level 2
Arginine	1.68(m), 3.73(t,6.5)	Level 2
Proline	4.07(dd,8.56,6.4)	Level 2
Cysteine	3.98(dd), 3.03(m)	Level 2
Carbohydrates		
Beta-glucose	4.58(d,7.8), 5.2(d,3.8)	Level 2
Alpha-glucose	4.63(d,7.9), 5.18(d,3.8)	Level 2
Sucrose	4.17(d,8.5), 5.4(d,3.8)	Level 1
Organic acids		
Malic acid	2.68(dd,16,4.1), 4.27(dd,10.1,2.7)	Level 2
Fumaric acid	6.56(s)	Level 2
Formic acid	8.46(s)	Level 2
Quinic acid	1.84(dd), 1.94(m)	Level 1
Succinic acid	2.59(s)	Level 2
Lactic acid	1.32(d), 4.1(q)	Level 2
Others		
Adenine	8.11(s), 8.21(s)	Level 2
Inositol	3.26(t,9.3), 4.00(t,2.8)	Level 2
Methyl salicylate	3.92(s), 10.74(s)	Level 2
Choline	3.22(s), 3.50(dd,5.8,4.1)	Level 2

Table S31: Secondary plant metabolites identified from ^{1}H NMR and 2D NMR spectra of M. charantia, with chemical shifts in ppm and the corresponding multiplicity m and scalar coupling J values (in Hz).

Metabolites	**Chemical shift (*m; J*)**	**Identification MSI**
Steroids		
Charantin*	0.85(s), 0.95(s), 1.01(s), 1.09(s), 1.25(s), 1.67(d,1)	Level 1
Momordicine	0.86-0.91(m), 6.06 (m), 1.25-1.35(m)	Level 2
Diosgenin	0.97(d,6.4), 1.02(s), 1.99(m), 3.36(t,10.5)	Level 2
Phenolics		
Gallic acid	7.06(s)	Level 2
Protocatechuic acid	6.92(d,8.2), 7.36(dd,8.77,3.14), 7.40(d,2.1)	Level 2
Gentisic acid	6.82(d,8.58), 6.98(dd,8.77,3.14), 7.29(d,3.14)	Level 2
Catechin	4.55(d,7.90), 2.5(dd,16.07,8.1), 2.84(dd,16.12,5.3)	Level 2
Vanillic acid	7.43(dd), 3.90(s), 6.94(d,8.24)	Level 1
Chlorogenic acid	7.17(d,1.8), 4.25(d,2.58), 3.89(dd), 2.13(m), 2.02(m)	Level 1
Syringic acid	7.03(s), 3.81(s)	Level 2
Epicatechin	4.28(m), 2.47(m), 2.91(m), 7.04(d,1.24), 6.12(d,2.1)	Level 2
Trans-ferulic acid	7.10(dd), 3.88(s), 6.37(d,15.96), 6.91(d,8.16)	Level 2
Benzoic acid	7.34(dd), 7.84(d), 7.54(t,7.33)	Level 2
Trans-cinnamic acid	7.77(m), 7.34(m), 6.52(d,16.06)	Level 2
Flavonoids		
Luteolin	6.55(s), 7.38(m), 6.20(d),6.43(d)	Level 2
Kaempferol	6.18(d,2.09), 8.10(m), 6.39(d,2.09), 6.90(m)	Level 2
Quercetin	6.82(d,8.57), 6.19(s), 6.41(s), 7.68(d,2.02)	Level 2
Naringenin	6.80(m), 7.30(m), 2.68(dd), 3.08(dd)	Level 2
Myricetin	6.18(d,2.09), 7.34(s), 6.37(d,2.09)	Level 2
Daidzein	7.96(d,8.75), 8.29(s), 6.81(m), 6.86(d,2.2)	Level 2
Isorhamnetin	7.72(d,2), 6.47(d), 9.74(s), 6.19(d)	Level 2

Note: The asterisk (*) symbol is showing that the compound charantin is a mixture of beta-sitosterol and stigmasterol together.

Table S32: Total phenolic and flavonoid content of seed, skin and pericarp of M. charantia. Data are expressed as mean ± SD.

	Seed	**Skin**	**Pericarp**
Phenolics (mg GAE / g DW)	324.88 ± 1.16	315.58 ± 1.16	320.23 ± 1.16
Flavonoids (mg QE / g DW)	151.85 ± 0.34	117.47 ± 3.47	161.46 ± 3.06

Table S33: Mean of EC_{50}(µg/mL) of DPPH radical scavenging activities of M. charantia fruit extracts (seed, pericarp and skin).

Extract	**EC_{50} (*µ*g/mL)**
Seed	94.21 ± 2.82
Pericarp	145.0 ± 4.35
Skin	245.0 ± 7.35

Table S34: ABTS assay measurements of antioxidant capacity of M. charantia fruit extracts (seed, pericarp and skin). Data are expressed as mean ± SD.

Extract	**EC_{50} (*µ*g/mL)**
Seed	124.99 ± 3.74
Pericarp	173.02 ± 5.19
Skin	262.67 ± 7.88

Table S35: Compounds present in M. charantia plant extracts identified using UPLC-ESI-MS in negative ionization mode.

Metabolites	**M.W.**	**$[M-H]^-$**	**R_t(min.)**
Epicatechin	290	289	0.674
Isorhamnetin	316	315	0.674
Beta-sitosterol	414	413	0.674
Catechin	290	289	5.909
Syringic acid	198	197	5.909
Stigmasterol	412	411	5.909

Table S36: List of metabolites with significantly altered concentrations in different parts of M. charantia plant extracts and their associated metabolic pathway.

Metabolic pathway	**Key metabolites**
Steroids metabolism	Charantin
	Momordicine
Phenylpropanoids and flavonoids metabolism	Catechin
	Chlorogenic acid
	Gallic acid
	Trans-ferulic acid
	Protocatechuic acid
	Vanillic acid
	Quercetin
	Luteolin
	Daidzein
	Kaempferol
	Myricetin
Amino acids metabolism	Alanine
	Cysteine
Choline metabolism	Choline

Table S37: Post-hoc analysis showing which groups are different given the p-value threshold of 0.05 for seed, skin and pericarp.

Metabolite	**p-value**	**-log10(p-value)**	**FDR**	**Fisher's LSD (Post-hoc tests)**
Quercetin	9.48*E* - 11	10.023	3.82*E* - 09	Seed - Pericarp; Pericarp - Skin; Seed - Skin
Kaempferol	1.27*E* - 09	8.8947	2.41*E* - 08	Seed - Pericarp; Pericarp - Skin; Seed - Skin
Alanine	1.64*E* - 07	6.7863	9.44*E* - 07	Skin - Pericarp; Skin - Seed
Chlorogenic acid	1.97*E* - 07	6.7061	1.08*E* - 06	Seed - Pericarp; Seed - Skin
Catechin	1.60*E* - 06	5.7947	7.22*E* - 06	Pericarp - Seed; Pericarp - Skin
Trans-ferulic acid	2.08*E* - 06	5.6819	9.00*E* - 06	Seed - Pericarp; Seed - Skin
Luteolin	3.78*E* - 06	5.4223	1.49*E* - 05	Pericarp - Skin; Seed - Skin
Protocatechuic acid	4.86*E* - 06	5.3130	1.86*E* - 05	Pericarp - Skin; Seed - Skin
Gallic acid	8.12*E* - 06	5.0903	2.90*E* - 05	Pericarp - Skin; Seed - Skin
GABA	1.43*E* - 05	4.8446	4.66*E* - 05	Seed - Pericarp; Pericarp - Skin; Seed - Skin
Vanillic acid	9.12*E* - 05	4.0401	2.47*E* - 04	Pericarp - Skin; Seed - Skin
Daidzein	3.86*E* - 04	3.4125	9.35*E* - 04	Pericarp - Skin; Seed - Skin
Myricetin	4.75*E* - 04	3.3232	1.09*E* - 03	Pericarp - Skin; Seed - Skin
Cysteine	1.10*E* - 03	2.9558	2.36*E* - 03	Pericarp - Skin
Beta-sitosterol	1.11*E* - 03	2.9535	2.36*E* - 03	Skin - Pericarp; Skin - Seed